

Quantum Hall ferromagnet in a parabolic well

G. M. Gusev, A. A. Quivy, T. E. Lamas, and J. R. Leite

Instituto de Física da Universidade de São Paulo, Caixa Postal 66318, 05315-970 São Paulo SP, Brazil

O. Estibals

*GHMFL, BP-166, F-38042 Grenoble Cedex 9, France
and INSA, F-31077 Toulouse Cedex 4, France*

J. C. Portal

*GHMFL, BP-166, F-38042 Grenoble Cedex 9, France,
INSA, F-31077 Toulouse Cedex 4, France
and Institut Universitaire de France, F-75005 Paris, France*

(Received 28 October 2002; published 21 April 2003)

We report the observation of an anomalous magnetoresistance peak in a tilted magnetic field corresponding to filling factor of 2 in several parabolic wells of different width. This phenomenon is due to the unpolarized-ferromagnetic transitions in quantum Hall ferromagnets. The domain formation induced by the random impurity potential is responsible for this magnetoresistance peak. The shift of the peak position with the tilt angle is attributed to the magnetic-field dependence of the exchange-correlation energy across the transition.

DOI: 10.1103/PhysRevB.67.155313

PACS number(s): 73.21.Fg, 72.20.My, 71.45.-d

I. INTRODUCTION

Lately, a broad class of phenomena related to the crossing of Landau levels with opposite spin orientation has been given much attention. The interest has been motivated by the close analogy between two-dimensional (2D) states in the quantum Hall regime and conventional electron ferromagnets. First, it has been noted that a 2D electron gas at Landau filling factor $\nu=1$ resembles a Heisenberg-like isotropic 2D ferromagnet, since electron-electron interactions lead to fully aligned electron spins in the limit of vanishing effective Lande g factor.¹ Such a ferromagnet can lose its ferromagnetic order at any finite temperature and therefore cannot be characterized by a transition temperature. Simple excitations (called skyrmions) of this strongly correlated ground state have been intensively studied theoretically² and experimentally^{3,4} in single GaAs/Al_xGa_{1-x}As layers and wells.

Another interesting example of the quantum Hall ferromagnet (QHF) is a bilayer 2D system based on two quantum wells separated by a tunneling barrier.⁵ In such a structure, the Landau levels in different layers can be characterized by a pseudospin index 1/2. Therefore, the state corresponding to isospin \uparrow is related to the electrons occupying the Landau level $n=0$ in the first well with a sub-band index $m=-1$, while the state with isospin \downarrow relates to the electrons occupying the $n=0$ level in the second quantum well with a sub-band index $m=+1$ (neglecting real spin). A bilayer system at total filling factor $\nu=1$ is equivalent to an easy-plane ferromagnet, since the pseudospin ferromagnetic order is found predominantly in the plane of the well. Such a QHF, in contrast to the isotropic case, undergoes a Kosterlitz-Thouless phase transition at a finite temperature. The physics becomes even richer when, in addition to the pseudospin, the real spin $\sigma=1/2$ is included. In this case, the QHF ground state depends on the nature of the crossing Landau levels. For example, at filling factor $\nu=2$, isospins \uparrow and \downarrow repre-

sent the states $n=0, \sigma=\uparrow, m=-1$, and $n=0, \sigma=\downarrow, m=+1$, respectively. When these states are brought close to degeneracy by applying an external electric field, the QHF ground state also corresponds to the easy-plane ferromagnet.⁶

Finally, the QHF has been observed in a single quantum well in tilted magnetic field.^{7-9,11} Since the electron orbital motion experiences only the perpendicular component of the magnetic field, the Landau-level splitting decreases with increasing the tilt angle. In addition, since the Zeeman splitting depends on the total magnetic field, the tilted-field experiments should demonstrate the coincidence of two Landau levels with opposite spins. In this case, at filling factor $\nu=2$, isospins \uparrow and \downarrow correspond to the states with $n=0, \sigma=\uparrow$, and $n=1, \sigma=\downarrow$, respectively. Theory predicts an easy-axis magnetic anisotropy each time Landau levels coincide in a tilted field.⁵ Such QHF also undergoes a first-order Ising-like transition with stronger thermodynamic anomalies than in the case of a Kosterlitz-Thouless transition in a bilayer system with a typical critical temperature ~ 1 K.

The transport properties of the QHF are not well understood. In an earlier work, it has been predicted that for crossing Landau levels in a single well the exchange interaction would lead to nonzero energy gaps through this transition.¹² The measurement of the activation energy of a 2D hole gas in a tilted field supported this prediction.⁸ However, another experiment demonstrated the disappearance of the $\nu=4$ minimum in GaAs quantum wells,⁹ a sharp reduction of the activation energy at $\nu=3,4$,¹⁰ or even hysteretic spikes in the resistance at filling factors $\nu=3,5,7$ in AlAs wells.¹¹ Such behavior can be attributed to the spatially random potential which always exists in quantum wells. Disorder leads to the variation of the effective Zeeman field acting on the pseudospins. This is expected to produce domains with particular pseudospin orientations.¹³ Several models consider transport through QHF samples in the presence of such domains and domain-wall loops. Some authors¹⁴ argued that the resistance spikes are due to the propagation of the electron quasiparti-

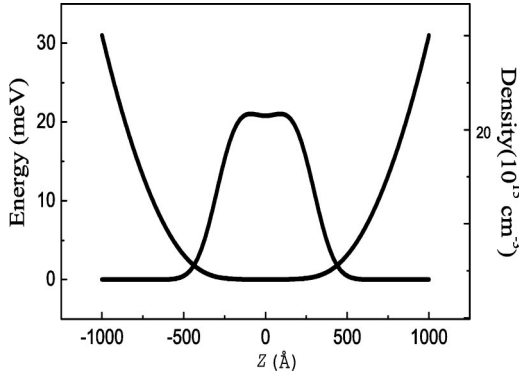


FIG. 1. Calculated total potential, electron density, and energy levels in a 2000 Å parabolic quantum well for a sheet density $n_s = 1.3 \times 10^{11} \text{ cm}^{-2}$.

cles (skyrmions) along the overlapping domain-wall loops. Since the Hartree-Fock approximation demonstrated the existence of an energy gap in the center of the domain wall, it was predicted that the resistivity spike should have an exponential temperature dependence. Chalker *et al.*¹⁵ suggested another gapless Ising-like domain-wall structure. Therefore, despite the several unusual magnetotransport observations and theoretical models, additional experiments with new systems are desirable in order to examine the possibility of an alternative explanation of the transport properties of the QHF.

In this work, we present the results of magnetotransport measurements in several parabolic quantum wells (PQW's) of different width. In wide PQW's with several occupied sub-bands, the energy difference between Landau levels in a strong magnetic field is determined by the energy-level spacing ΔE_{ij} in zero field, which is much smaller than $\hbar\omega_c$ (ω_c is the cyclotron frequency). Therefore, it is expected that the coincidence of Landau levels with opposite spin may occur at small tilt angles. This coincidence corresponds to the quantum Hall easy-axis Ising ferromagnet.

II. WIDE PARABOLIC WELLS IN A TILTED MAGNETIC FIELD

The first wide parabolic wells were grown by Sundaram *et al.*¹⁶ and by Shayegan *et al.*¹⁷ The parabolic variation of the well potential was introduced in order to avoid the soft barrier in the center originating from Coulomb interaction among electrons in a wide quantum well. This makes it possible to create a quasi-three-dimensional electron system with several occupied sub-bands. Figure 1 shows the example of a self-consistent calculation for a partially filled 2000 Å $\text{Al}_x\text{Ga}_{1-x}\text{As}$ parabolic well with the electronic slab width $W_e \approx 600$ Å and the sheet density $1.3 \times 10^{11} \text{ cm}^{-2}$. In this case, two sub-bands are occupied.

The problem of a quasi-three-dimensional electron gas in a tilted magnetic field was solved analytically for a parabolic well by Merlin *et al.*¹⁸ The energy of the electrons in a parabolic quantum well with the potential $V=(az)^2$ and in a tilted magnetic field is given by

$$E = E_\alpha(n_\alpha + 1/2) + E_\beta(n_\beta + 1/2), \quad (1)$$

$$E_\alpha = [(\hbar\omega_c \cos \alpha)^2 + (\hbar\Omega \sin \alpha)^2 - (\hbar\omega_c)(\hbar\Omega) \sin(2\alpha) \sin \Theta]^{1/2}, \quad (2)$$

$$E_\beta = [(\hbar\omega_c \sin \alpha)^2 + (\hbar\Omega \sin \alpha)^2 + (\hbar\omega_c)(\hbar\Omega) \sin(2\alpha) \sin \Theta]^{1/2}, \quad (3)$$

where $\Omega = a(2/m)^{1/2}$, $\omega_c = eB/mc$, m is the effective mass, n_α and n_β are integers, and Θ is the tilt angle between the magnetic field and the normal to the parabolic-well plane z . The angle of rotation α can be obtained from another equation

$$\tan(2\alpha) = (\hbar\Omega)(\hbar\omega_c) \sin \Theta / [(\hbar\Omega)^2 - (\hbar\omega_c)^2]. \quad (4)$$

Figure 2 demonstrates the evolution of the Landau levels (LL) belonging to different sub-bands of a $W_e = 600$ Å parabolic well in a perpendicular magnetic field, when B is tilted away from z (neglecting spin splitting). It must be emphasized here that the levels in a strong magnetic field consist of the electronic sub-bands belonging to the $n=0$ Landau level. The energy spacing is described by the formula

$$\Delta E_{ij} = \hbar\Omega \cos \Theta, \quad (5)$$

and therefore diminishes with increasing tilt angles. However, a full PQW is more similar to a square quantum well than to a harmonic potential. In this case, the energy spectrum E_i of a PQW in a zero magnetic field can be roughly approximated by the spectrum of a square well $E_i = i^2(\hbar/W)^2/8m$ with a width equal to that of the electron layer, but the energy-level structure in the presence of a tilted magnetic field cannot be obtained analytically. However, in the limit of strong magnetic field, where the magnetic length $l_B = \sqrt{\hbar c/eB} \ll W_e$, the energy spacing is proportional¹⁹ to $\cos^2 \Theta$. Figure 2 shows that, in a quasi-parallel magnetic field, the two-dimensional Landau states collapse into a

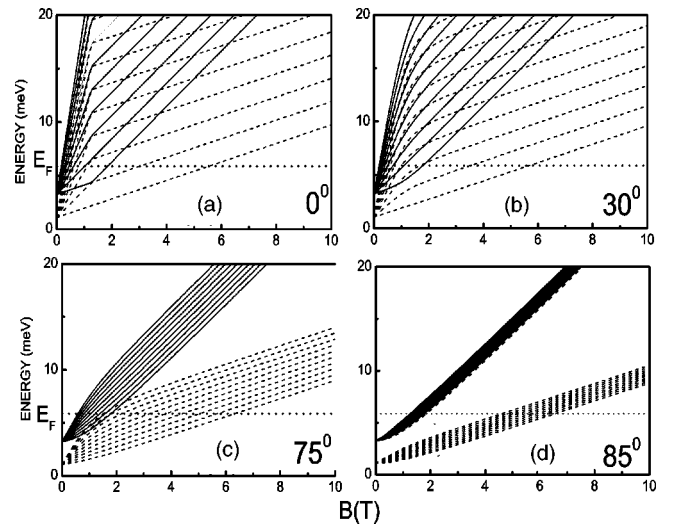


FIG. 2. Energy of a wide (2000 Å) parabolic quantum well as a function of the magnetic field for different tilt angles Θ . The position of the Fermi level at zero magnetic field is shown by the dotted line. Ten Landau levels for each sub-band are shown. Spin splitting is neglected.

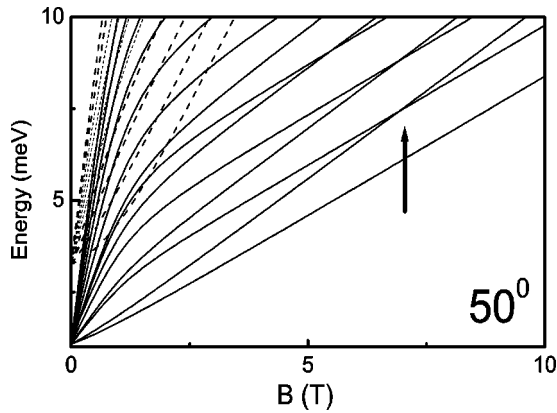


FIG. 3. Diagram of the Landau levels in a wide (2000 Å) parabolic quantum well as a function of the magnetic field for $\Theta = 50^\circ$. The Zeeman splitting for the three lowest levels is included. The level crossing at $\nu=2$ is shown by an arrow.

single 3D Landau state. However, the degeneracy of the oblique states depends only on the magnetic-field component perpendicular to the quantum well plane and equal to eB_\perp/hc . Therefore, it is expected that, for large tilt angles in the strong magnetic-field regime corresponding to the Landau filling factor $\nu=1,2$, the quantum Hall effect behavior should resemble the behavior in a parallel magnetic field, if only the normal component of the field is taken into account. Indeed, the three-dimensional limit may be reached when $\Theta \rightarrow 90^\circ$ and the distance between the two-dimensional Landau sub-bands $\Delta E_{ij} \rightarrow 0$, as can be seen in Fig. 2(c). In a real system, the energy levels have a finite width due to the disorder Γ , and therefore the system has a 3D energy spectrum when the electron sub-bands overlap, $\Gamma \sim \Delta E_{ij}$, which probably occurs in the interval $\Theta \sim 85^\circ - 90^\circ$. If we include spin splitting into this picture, we may expect the coincidence of two Landau levels with opposite spin. Figure 3 shows schematically such a level crossing at $\Theta = 50^\circ$. It must be emphasized here that the effective mass and the effective g factor in GaAs are such that the Zeeman splitting is roughly 1/60 of the LL spacing. Therefore, in GaAs quantum wells, the angle at which the Landau level coincidence occurs is close to 80° . Such limitations lead to the fact that the first observation of the level coincidence has been reported for electrons in $\text{Ga}_x\text{In}_{1-x}\text{As}/\text{InP}$ structures⁷ and for 2D holes in $\text{GaAs}/\text{Al}_x\text{Ga}_{1-x}\text{As}$ heterostructures⁸ which have a large effective “bare” g factor. In $\text{Al}_x\text{Ga}_{1-x}\text{As}$, the g factor increases monotonically from $g = -0.44$ at $x=0$ (GaAs) to $g \approx +0.5$ at $x=0.35$, vanishing around $x \approx 0.13$.²⁰ In our $W_e = 800\text{-\AA}$ parabolic well, the average g factor is -0.24 and corresponds to a Zeeman energy $\Delta E_Z = 0.118$ meV at $B = 8.5$ T. When the width of the well increases, the coincidence of two LL should be observed at a smaller tilt angle.

III. EXPERIMENTAL RESULTS

The samples were grown in a Gen II system by molecular-beam epitaxy on top of GaAs(001) substrates. After oxide desorption, a 2000-Å-thick GaAs buffer was deposited, followed by a superlattice containing ten periods of

$(\text{AlAs})_5/(\text{GaAs})_{10}$, a 5000-Å-thick GaAs buffer, a 500-Å-thick $\text{Al}_{0.29}\text{Ga}_{0.81}\text{As}$ barrier, the PQW with an aluminum content ranging from 0.29 to 0, a second 500-Å-thick $\text{Al}_{0.29}\text{Ga}_{0.81}\text{As}$ barrier and a 100-Å-thick GaAs cap layer. Several samples were grown with a PQW width ranging from 1000 to 3000 Å and symmetrically doped with a silicon δ spike located at 150 Å from their border. The whole structure was grown at 580°C . The mobility of the electron gas in our samples was of the order of $(70-100) \times 10^3$ cm^2/Vs and the density was $(1-2) \times 10^{11}$ cm^{-2} . As a consequence, our PQW’s were only partially full with two to three occupied sub-bands. The electron sheet density was varied by illumination with a red light-emitting diode. At high electron density, the resistance in the minimum of the quantum Hall effect became very high, because the energy spacing ΔE decreases with density, and the Landau levels overlap. In the present paper, we focus on the low-density results. Transport measurements in wide PQWs with high electron density and results in parallel magnetic fields were reported in previous papers.²¹ The samples were processed into Hall bars with a width $d = 100$ μm and a distance between the voltage probes $L = 200$ μm . Four-terminals resistance R_{xx} and Hall R_{xy} measurements were carried out down to 50 mK in a magnetic field up to 15 T. The samples were immersed in a mixing chamber of a top-loading dilution refrigerator with an ac current not exceeding 10^{-7} A. We measured the magnetoresistance at different angles Θ between the field and the normal to the sample, rotating our sample *in situ*. Figure 4 shows the magnetoresistivity traces in a perpendicular and tilted magnetic field for angles $\Theta < 50^\circ$. In magnetic fields $B > 2$ T, we observe the typical quantum Hall effect behavior. It is worth noting that the minimum in R_{xx} at $B = 4.3$ T corresponds to the gap between the $n=0$ and $n=1$ (LL filling factor $\nu=2$) spin resolved Landau levels. In magnetic fields such as $1 \text{ T} < B < 2 \text{ T}$, we can observe the anticrossing of Landau levels belonging to different sub-bands, as already reported by Ensslin *et al.*²² However, as expected, the magnetoresistance peaks in stronger magnetic fields are not shifted, and their position is determined by the normal component of the magnetic field $B \cos \Theta$. Surprisingly, this picture changes at larger tilt angles (Fig. 5): in the interval $55^\circ < \Theta < 68^\circ$ and for magnetic fields corresponding to the filling factor $\nu=2$, an additional anomalous peak appears between two magnetoresistance peaks. Figure 5 also shows a gray-scale presentation of the magnetoresistivity traces as a function of the total magnetic field B_{tot} . We can see that the anomalous peak occurs at $B_{\text{total}} = 8.9$ T and does not move with the angle. This peak was not related to a step in the Hall resistance. Figure 6(a) shows the longitudinal and Hall resistance as a function of the normal component of the magnetic field for two tilt angles $\Theta = 0^\circ$ (perpendicular magnetic field) and $\Theta = 60^\circ$, when the anomalous peak is located exactly between the $\nu=3/2$ and $\nu=5/2$ peaks. Figure 6(b) shows the transverse and Hall conductivity σ_{xx} and σ_{xy} recalculated from the resistivities. We can see that the plateau in σ_{xy} is slightly distorted where the anomalous peak appears in σ_{xx} , but there is clearly no evidence of any step. The coincidence of the Landau level with opposite spin is expected to occur at

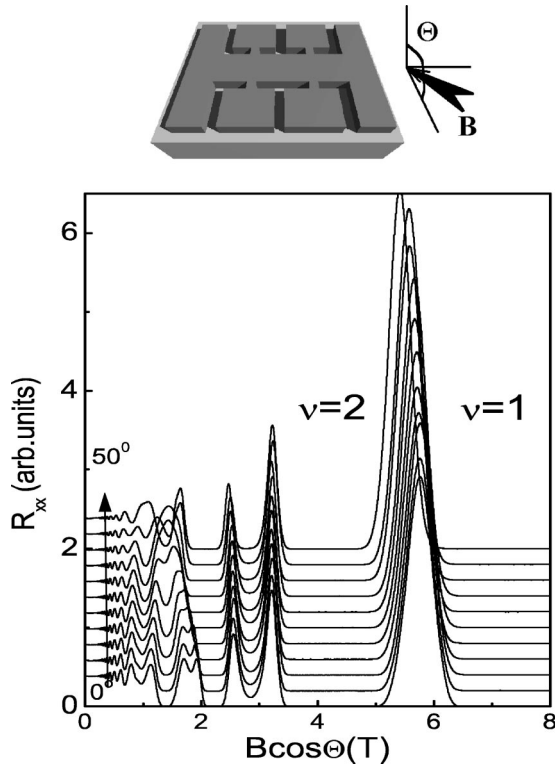


FIG. 4. Magnetoresistance of a 2000 Å PQW as a function of the normal component of the magnetic field for different tilt angles Θ at $T=50$ mK. The in-plane magnetic-field component is directed along the y axis, perpendicular to the current flow. Top—Schematic view of the sample and experiment geometry.

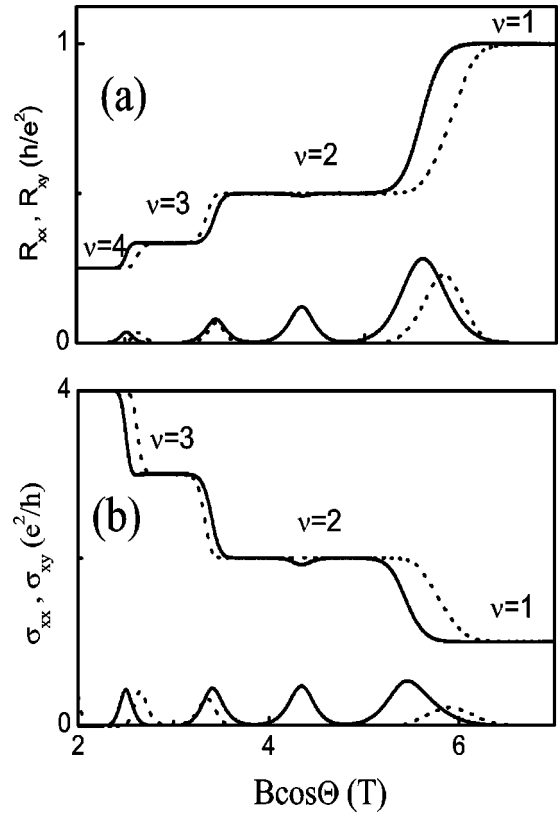


FIG. 6. Longitudinal R_{xx} and transverse R_{xy} resistance (a) and longitudinal σ_{xx} and transverse σ_{xy} conductance (b) of a 2000 Å PQW as a function of the magnetic field at $\Theta=0^\circ$ (dashes) and $\Theta=60^\circ$. $T=50$ mK.

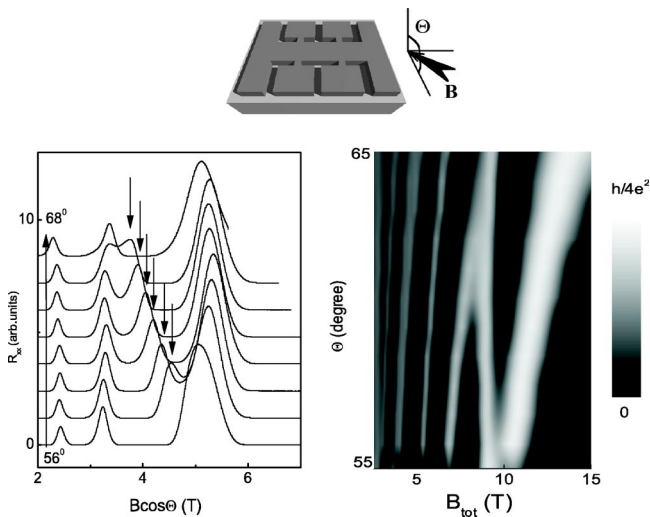


FIG. 5. Left—magnetoresistance of a 2000 Å PQW as a function of the normal component of the magnetic field for different tilt angles $56^\circ < \Theta < 68^\circ$ at $T=50$ mK. The arrows indicate the anomalous resistance peak. Top—schematic view of the sample and experiment geometry. Right—gray-scale presentation of the tilt-angle dependence of the magnetoresistance on the total magnetic field. $T=50$ mK.

a lower total magnetic field in the samples with a larger well width. This tendency was indeed observed in PQW's with different geometric width W . Figure 7 shows a gray-scale presentation of the magnetoresistivity traces as a function of the total magnetic field B_{tot} for a sample with $W=2500$ Å. The anomalous peak occurs at $B_{tot}=6.8$ T and slightly moves to larger tilt angles. Figure 8 illustrates the summary of the position of the anomalous peak. In all the samples, the anomalous peak at $\nu=2$ occurs at a critical magnetic field B_{tot}^c that depends on the “bare” well width W . It is worth

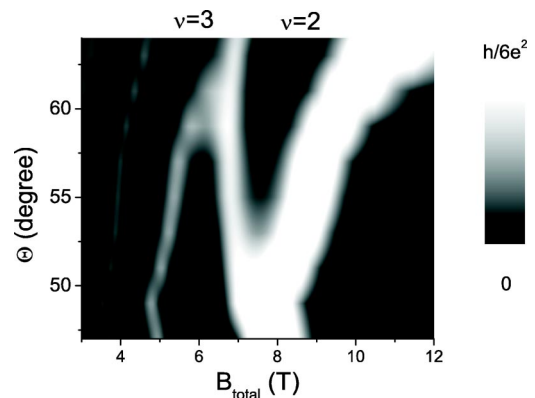


FIG. 7. Gray-scale presentation of the tilt-angle dependence of the magnetoresistance of a 2500 Å PQW on the total magnetic field. $T=50$ mK.

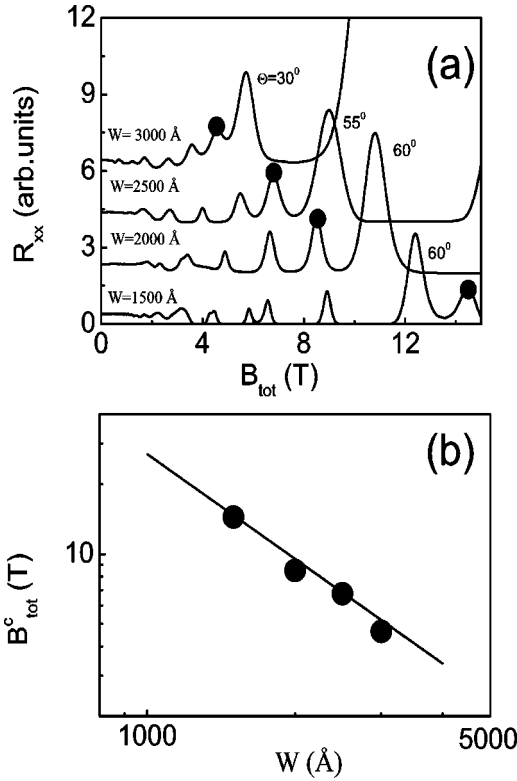


FIG. 8. (a) R_{xx} as a function of the total magnetic field for PQW's with different geometrical widths W . $T=50$ mK. The curves are shifted for clarity. The circles show the anomalous peak corresponding to the ferromagnetic transition at $\nu=2$. (b) Critical magnetic field corresponding to the ferromagnetic transition at $\nu=2$ as a function of the sample width. Solid line— $B_{total}^c \sim W^{-1.5}$ dependence.

noting here that, in our experiments, the width of the electronic slab W_e is 2–3 times smaller than the bare well width, resulting in partially filled PQW's (see, for example, Fig. 1). The electron sheet density n_s was varied by illumination with a red light-emitting diode. Surprisingly, we found that the value of the field B_{total}^c does not change with n_s and, consequently, with W_e . This observation is not consistent with the expected behavior, since the difference of energy ΔE is much more influenced by the electronic slab width W_e than by W . This discrepancy will be discussed in the following section. We may also summarize the electron sheet density dependence in the following way. In 2D systems, the Landau filling factor is determined by the simple equation $\nu = n_s 2\pi\hbar c / eB_{total} \cos \Theta$. Since the anomalous peak occurs at $\nu=2$, we can obtain the electron density when the peak is observed exactly in the middle of the minima (corresponding to $\nu=2$), yielding $n_s = eB_{total}^c \cos \Theta / \pi\hbar c$. Figure 9 demonstrates such a behavior. We may see that the experimental points fit Landau filling factor angle dependence, which means that B_{total}^c for parabolic well with fixed geometrical width W does not depend on the electron sheet density.

IV. QUANTUM HALL FERROMAGNET STATES IN A SINGLE WELL

Let us focus now on the possible explanation of the anomalous resistance peaks at $\nu=2$. A single-electron pic-

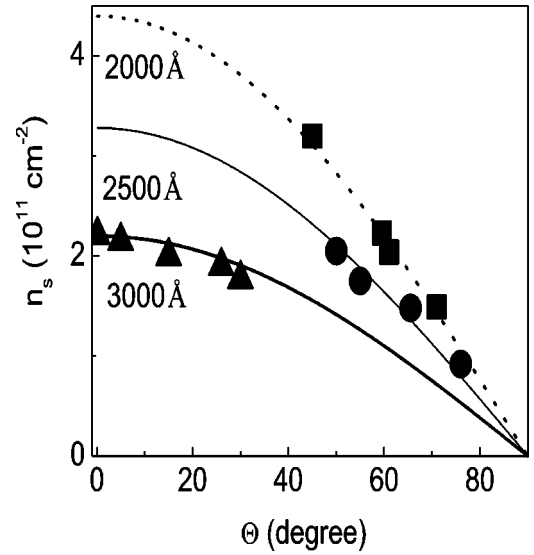


FIG. 9. Electron sheet density versus tilt angle corresponding to the ferromagnetic transition at $\nu=2$ for PQW's with different widths. Lines— $n_s = eB_{total}^c \cos \Theta / \pi\hbar c$.

ture predicts the disappearance of the minima when the bare energy levels cross. From the measurement of the activation energy at $\nu=2$, we found that the energy spacing follows a $\cos \Theta$ dependence on the tilt angle. This corresponds to the condition

$$\Delta E \cos \Theta - g \mu_B B_{total} = \Delta E B_{\perp} / B_{total} - g \mu_B B_{total} = 0. \quad (6)$$

We obtain the energy spacing ΔE from the measurement of the electron sheet density in the first and second sub-bands, that can be found from the Shubnikov de Haas oscillations measured at low magnetic field.²³ Using Eq. (6) and the value of $B_{total}^c = 8.9$ T for the data shown in Fig. 4, we get $g \approx 2.4$ which is much larger than the expected bare g factor in that PQW ($g=0.14$, see Sec. II). However, in a realistic picture, the effective interaction between pseudospins should be included. For pseudospin Landau levels crossings, Eq. (6) should be modified as

$$\Delta E \cos \Theta - g \mu_B B_{total} = \Delta E B_{\perp} / B_{total} - g \mu_B B_{total} = -U_{\sigma,\sigma}, \quad (7)$$

where $U_{\sigma,\sigma}$ is the exchange term that produces an easy-axis anisotropic QHF.⁵ Therefore, the Landau levels might be closer to degeneracy at a smaller tilt angle than is expected for bare energy levels, even in a perpendicular magnetic field, as we found for our 3000 Å sample (Figs. 8 and 9). Using Eq. (7) and the results from the 2000 Å and 2500 Å PQW, we deduced the exchange-correlation energy term as a function of the perpendicular magnetic field. Figure 10 shows $|U_{\sigma,\sigma}|$ versus B_{\perp} and it can be seen that its dependence is linear. It is worth noting that the same linear dependence has been observed in AlAs quantum wells.¹¹ The effective Coulomb interaction has been calculated for double and single quantum well structures by Jungwirth *et al.*⁹ For $\nu=2$ in a narrow ($W=430$ Å) quantum well with a single occupied sub-band, $U_{\sigma,\sigma}$ is negative and equal to $0.04e^2/\epsilon l_H = 0.432B_{\perp}^{1/2}(\text{T})(\text{meV})$. Figure 10 shows that the

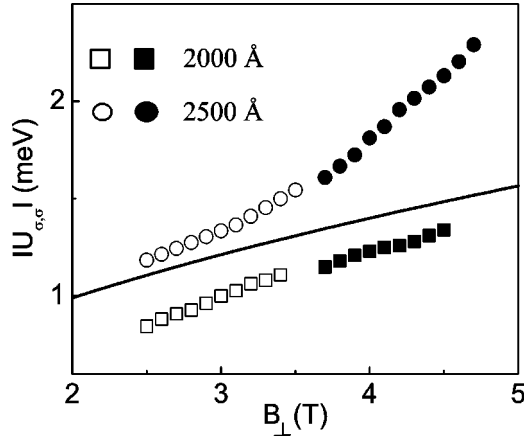


FIG. 10. Exchange-correlation energy extracted from Eq. (7) and from the data shown in Figs. 5 and 7 for various densities (empty circles $n_s = 1.49 \times 10^{11} \text{ cm}^{-2}$, full circles $n_s = 2.1 \times 10^{11} \text{ cm}^{-2}$, empty squares $n_s = 1.49 \times 10^{11} \text{ cm}^{-2}$, full squares $n_s = 1.75 \times 10^{11} \text{ cm}^{-2}$). Solid line— $|U_{\sigma,\sigma}| \sim 0.7B_{\perp}^{1/2}$ dependence.

curve behaves as $|U_{\sigma,\sigma}| \approx 0.7B_{\perp}^{1/2}(\text{T})$ (meV). This result is somewhat surprising, since the exchange-correlation energy term is drastically reduced for wide wells.²⁴ The linear dependence of $|U_{\sigma,\sigma}|$ on B_{\perp} instead of $B_{\perp}^{1/2}$ is also not very clear. Calculations²⁴ demonstrated that the correlation energy follows the formula

$$|U_{\sigma,\sigma}| \approx 1.8B_{\perp}^{1/2}(\text{T}) / (W_e/l_B + 0.36) (\text{meV})$$

Moreover, when $W_e/l_B \gg 0.3$ (in our case it occurs for $B > 1$ T), the exchange correlation energy is saturated $|U_{\sigma,\sigma}| \approx 0.64$ meV and does not depend anymore on the magnetic field, which is not consistent with our data. Equation (7) may explain the absence of the magnetic transition at higher filling factor, for example, at $\nu = 4$. The energy spacing ΔE has the same value at $\nu = 4$ (see Fig. 2), in contrast to $U_{\sigma,\sigma}$ that is probably inversely proportional to the number of occupied polarized levels.¹¹ In this case, the smaller exchange energy can bring the up and down pseudospin Landau levels close to degeneracy only at large tilt angles. It must be emphasized that in PQW's, the effective g factor is very small. Therefore, the second term in Eq. (7), which corresponds to the bare Zeeman splitting, is small in comparison with the exchange-correlation energy term. However, it may lead to a nonzero value of $|U_{\sigma,\sigma}|$ in $B_{\perp} = 0$. We attribute this small discrepancy to the approximate character of Eq. (7) which is valid only in a strong perpendicular magnetic field, when the spin splitting is resolved. Neglecting the Zeeman term, we may rewrite Eq. (7) in the form

$$B_{total} \approx \Delta E B_{\perp} / |U_{\sigma,\sigma}|.$$

Since $|U_{\sigma,\sigma}| \sim B_{\perp}$, we obtain $B_{total} \sim \Delta E$. For a PQW, $\Delta E \sim W_e^{-1}$, yielding $B_{total} \sim W_e^{-1}$. From our experiments, we find that $B_{total} \sim W^{-1.5}$ (see Fig. 8) and B_{total} does not depend on the electronic slab width W_e and the electron sheet density (Fig. 9). We may attribute this discrepancy to the complex character of the energy spectrum of a PQW in a strong magnetic field. Numerical calculations²⁵ demonstrated

that the Hartree term and the exchange-correlation term might change the well potential in a magnetic field and lead to redistribution of the charge between the sub-bands. Therefore, the energy spacing ΔE in a strong field will be more sensitive to the PQW parameters (such as the width of the bare parabola) than to the electron density. To conclude this part, we have argued that the behavior of the anomalous peak in the magnetoresistance is in qualitative agreement with the simple model described by Eq. (7). The quantitative explanation of the correlation-energy dependence on the perpendicular magnetic field and the sample width requires a detailed theoretical investigation.

We now turn to the transport properties of the QHF. Previous experiments⁶⁻⁸ did not allow one to make definitive conclusions about the transport mechanism in a QHF. Only the recent observation of the resistance spikes in single AlAs wells¹¹ and large resistance anisotropy in wide GaAs wells²⁷ and Si/GeSi heterostructures²⁸ in tilted magnetic fields stimulated discussions about the origin of the observed transport anomalies.¹⁵ As has been argued by Falko and Iordanskii,¹³ disorder arising from the density inhomogeneities produces a multidomain structure. Therefore, transport in a QHF is attributed to the diffusion along the network formed by the domain walls in analogy with transport in integer quantum Hall effect. However, in contrast to quantum Hall systems where transport is associated with electrons, in QHF the current-carrying states are quasiparticles denominated skyrmions. In ordinary thin-films magnets, skyrmions can exist, in principle, but they are not important because they do not carry charge. In a QHF, skyrmions carry charge and can be observed in transport experiments⁴ at $\nu = 1$. At $\nu = 2$, pseudoskyrmions are formed due to the alignment of the pseudospins, and therefore they are still the excitation states which form the main propagating modes along the domain walls of the QHF. The structure of the domain wall is discussed in different models. Jungwirth and McDonald¹⁴ argued that, for a Blocklike domain-wall structure, the transport should be due to the activation through the quasiparticle excitation gap $\sim 2-4$ K. This explains the decrease of the spike at $\nu = 3$ with temperature in AlAs quantum wells.¹¹ However, the activation energy of different spikes has not been measured in Ref. 11 and therefore the understanding of the physics of domains in a QHF still needs further theoretical and experimental investigations. In our samples, we found magnetoresistance peaks rather than narrow spikes as observed in AlAs wells.¹¹ It is worth noting that the nonzero longitudinal resistance in the conventional quantum Hall regime is currently understood in terms of percolation through different regions of the samples, along the contours of the disordered potential. Percolation occurs when the Fermi energy coincides exactly with the center of the Landau levels. The percolation threshold is equivalent to the one of a network where the transmission coefficient of each saddle point in the random potential is equal to 1/2. This gives the value of the conductivity peaks between plateaus $\sigma_{xx} = e^2/2h$ and the Hall conductivity $\sigma_{xy} = (e^2/h)(N + 1/2)$. We see in Fig. 5(b) that all four peaks observed in a tilted magnetic field at $B > 2$ T have a value close to the universal value $e^2/2h$. This might be an indication that the anomalous peaks are due to

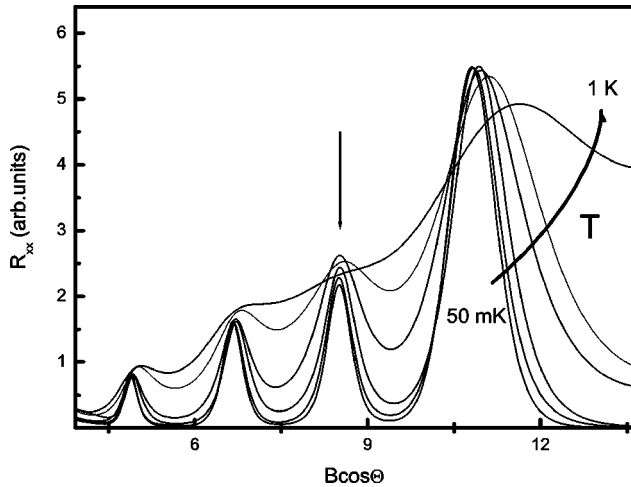


FIG. 11. Longitudinal resistance R_{xx} of a 2000 Å PQW as a function of the magnetic field at $\Theta = 60^\circ$ for different temperatures. The arrow indicates the anomalous magnetoresistance peak.

percolation through the samples, like the quantum Hall σ_{xx} peaks. This is not surprising because, as was mentioned above, the network of the domain walls might be generated by the same disorder potential as the percolation network in the quantum Hall regime. We also measured the temperature dependence of the anomalous peak in a tilted magnetic field, as shown in Fig. 11. We see that the peak does not depend on the temperature and its behavior resembles the one of the quantum Hall R_{xx} peaks. It is worth noting that we observe a similar behavior in all the PQW's of different width and with different sheet electron densities. The strong temperature dependence of the peak in AIAs can be attributed to the incomplete formation of the domain-wall network. The percolation nature of the anomalous peak in our QHF can be justified by the model considered in Ref. 15 where the Ising-like domain-wall structure has been proposed that led to a temperature-independent percolation of the two counter-propagating sets of modes along the domain walls. Such a network resembles the percolation contour in the random magnetic-field problem which leads to zero Hall conductance.²⁶ This explains the absence of the step in the Hall resistance across the transition (Fig. 6). It has to be mentioned that the model¹⁵ describes also the transport anisotropy observed in Si/Ge heterostructure and GaAs wide wells.^{27,28} In these structures, the domain-wall network should be strongly anisotropic due to the sample-surface roughness. We did not find such an anisotropy in our PQW's and, indeed, it agrees with the model considered in Ref. 15. Since a QHF has been observed in Refs. 27 and 28 at very large tilt angles ($\sim 80^\circ$), any small variation of the surface

corrugation leads to the variation of the local angle by 0.5° and, consequently, to the variation of the local effective magnetic field by 20%. In our PQW's, the QHF is observed at $\Theta = 60^\circ$ (see Fig. 6), and the same variation of the local tilt angle leads to a 0.8% fluctuation of the local effective magnetic field. Such a small variation is not enough to produce an anisotropy in the domain-wall transport. It will be interesting to look for an anisotropy in our samples with a lower density, where the QHF should be observed at higher tilt angles, or in artificially corrugated samples.²⁹

Finally, we discuss the hysteresis behavior observed in some works.^{6,11} Such a hysteresis behavior is reported as a proof of the existence of the domain structure in QHF samples. Hysteresis occurs because the domain may arise in the metastable states. In this case, the domain-wall network will depend on the direction of the magnetic-field sweep. Another origin of the domain is disorder, as already discussed above. Such domain might be stable, and no hysteresis behavior appears in this case. We did not find hysteresis in our samples down to 50 mK.

V. CONCLUSION

We have demonstrated that a parabolic quantum well is a promising system for understanding the physics of quantum Hall ferromagnets. The magnetic transition can be controlled by the variation of the PQW width. In comparison with the previous studies of a QHF in GaAs and AIAs single wells, the transition in our PQW is characterized by a reproducible peak in the longitudinal magnetoresistance. In wide parabolic wells a QHF is observed in perpendicular magnetic field and can be tuned by the variation of the electron sheet density. This makes it possible to study the physics of magnetic domains in a QHF. In particular, we found that the behavior of the anomalous peak resembles the typical behavior of the magnetoresistance peak in a quantum Hall insulator-Hall metal transition. We attribute such a behavior to percolation along the domain walls with an Ising-like structure. We also found that the anomalous peak moves from low filling factor to high ν with increasing tilt angle Θ . Qualitatively, it can be explained by the increase of the exchange-correlation energy with B_\perp . Since the Zeeman splitting in our system is very small, the exchange energy is comparable with the energy-level separation in our PQW's.

ACKNOWLEDGMENTS

The authors thank V. I. Falko for useful discussions and C. S. Sergio for assistance with the sample preparation. Support of this work by FAPESP, CNPq (Brazilian agencies), and USP-COFECUB is acknowledged.

¹*The Quantum Hall Effect*, edited by R. E. Prange and S. M. Girvin (Springer-Verlag, New York, 1990).

²S.L. Sondhi, A. Karlhede, S.A. Kivelson, and E.H. Rezayi, *Phys. Rev. B* **47**, 16 419 (1993).

³R. Tycko, S.E. Barret, G. Dabbagh, and L.N. Pfeiffer, *Science*

268, 1460 (1998).

⁴D.K. Maude *et al.*, *Phys. Rev. Lett.* **77**, 4604 (1996).

⁵T. Jungwirth and A.H. MacDonald, *Phys. Rev. B* **63**, 035305 (2000).

⁶V. Piazza *et al.*, *Nature (London)* **402**, 638 (1999).

- ⁷S. Koch, R.J. Haug, K.V. Klitzing, and M. Razeghi, *Phys. Rev. B* **47**, 4048 (1993).
- ⁸A.J. Daneshvar *et al.*, *Phys. Rev. Lett.* **79**, 4449 (1997).
- ⁹T. Jungwirth *et al.*, *Phys. Rev. Lett.* **81**, 2328 (1998).
- ¹⁰K. Muraki, T. Saku, and Y. Hirayama, *Phys. Rev. Lett.* **87**, 196801 (2001).
- ¹¹E.P. Poortere, E. Tutuk, S.J. Papadakis, and M. Shayegan, *Science* **290**, 1546 (2000).
- ¹²G.F. Giuliani and J.J. Quinn, *Phys. Rev. B* **31**, 6228 (1985).
- ¹³V.I. Falko and S.V. Iordanskii, *Phys. Rev. Lett.* **82**, 402 (1999).
- ¹⁴T. Jungwirth and A.H. MacDonald, *Phys. Rev. Lett.* **87**, 216801 (2001).
- ¹⁵J.T. Chalker, D.G. Polyakov, F. Evers, A.D. Mirlin, and P. Wölfle, *Phys. Rev. B* **66**, 161317 (2002).
- ¹⁶M. Sundaram, A.C. Gossard, J.H. English, and R.M. Westervelt, *Superlattices Microstruct.* **4**, 683 (1988).
- ¹⁷M. Shayegan, T. Sajoto, M. Santos, and C. Silvestre, *Appl. Phys. Lett.* **53**, 791 (1988).
- ¹⁸R. Merlin, *Solid State Commun.* **64**, 99 (1987).
- ¹⁹V.I. Falko, *Solid State Commun.* **78**, 925 (1991).
- ²⁰C. Weisbuch and C. Hermann, *Phys. Rev. B* **15**, 816 (1977).
- ²¹C.S. Sergio, G.M. Gusev, J.R. Leite, E.B. Olshanetskii, A.A. Bykov, N.T. Moshegov, A.K. Bakarov, A.I. Toropov, D.K. Maude, O. Estibals, and J.C. Portal, *Phys. Rev. B* **64**, 115314 (2001); G.M. Gusev, A.A. Quivy, T.E. Lamas, J.R. Leite, A.K. Bakarov, A.I. Toropov, O. Estibals, and J.C. Portal, *ibid.* **65**, 205316 (2002).
- ²²K. Ensslin, A. Wixforth, M. Sundaram, P.F. Hopkins, J.H. English, and A.C. Gossard, *Phys. Rev. B* **47**, 1366 (1993).
- ²³E.G. Gwinn, R.M. Westervelt, P.F. Hopkins, A.J. Rimberg, M. Sundaram, and A.C. Gossard, *Phys. Rev. B* **39**, 6260 (1989).
- ²⁴D. Lilliehöök, *Phys. Rev. B* **62**, 7303 (2000).
- ²⁵C.E. Hembree, B.A. Mason, A. Zhang, and J.A. Slinkman, *Phys. Rev. B* **46**, 7588 (1992).
- ²⁶Y.B. Kim, A. Furusaki, and D.K.K. Lee, *Phys. Rev. B* **52**, 16 646 (1995).
- ²⁷W. Pan *et al.*, *Phys. Rev. B* **64**, 121305 (2001).
- ²⁸U. Zeitler, H.W. Schumacher, A.G.M. Jansen, and R.J. Haug, *Phys. Rev. Lett.* **86**, 866 (2001).
- ²⁹G.M. Gusev, J.R. Leite, A.A. Bykov, N.T. Moshegov, V.M. Kudryashev, A.I. Toropov, and Yu.V. Nastaushev, *Phys. Rev. B* **59**, 5711 (1999); A.A. Bykov, G.M. Gusev, J.R. Leite, A.K. Bakarov, A.V. Goran, V.M. Kudryashev, and A.I. Toropov, *ibid.* **65**, 035302 (2001).